ChemComm

Accepted Manuscript

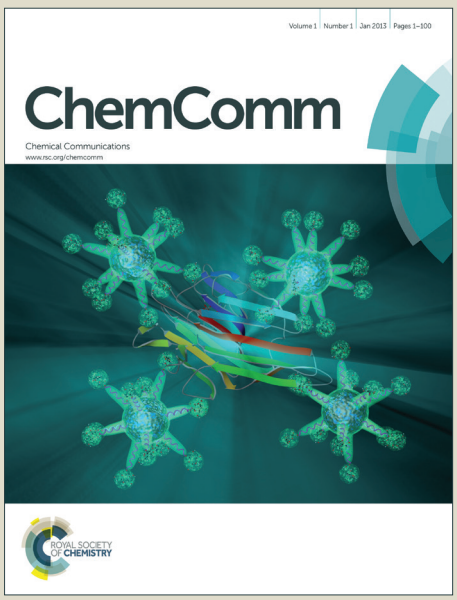

ROYAL SOCIETY OF CHEMISTRY

www.rsc.org/chemcomm

Cite this: DOI: 10.1039/c0xx00000x

www.rsc.org/xxxxxx

COMMUNICATION

Ultralow-Temperature CO Oxidation on In_2O_3-Co_3O_4 Catalyst: A Strategy to Tune CO Adsorption Strength and Oxygen Activation Simultaneously

Yang Lou[a+], Xiao-Ming Cao[a+], Jinggang Lan[a], Li Wang[a], Qiguang Dai[a], Yun Guo[a*], Jian Ma[a], Zhenyang Zhao[a], P. Hu[a,b] and Guanzhong Lu[a]

Received (in XXX, XXX) Xth XXXXXXXXX 20XX, Accepted Xth XXXXXXXXX 20XX
DOI: 10.1039/b000000x

Highly efficient In_2O_3-Co_3O_4 catalysts were prepared for ultralow-temperature CO oxidation by simultaneously tuning the CO adsorption strength and oxygen activation over Co_3O_4 surface, which could completely convert CO to CO_2 at as low as -105 °C compared to -40 °C over pure Co_3O_4, and the stability was greatly promoted.

Low-temperature CO oxidation has drawn great attention due to not only its wide applications but also its simplicity as a good model reaction to develop and test the novel catalyst [1-9]. Gold catalyst made a breakthrough in low-temperature catalysis [5, 8-10], which could completely convert CO to CO_2 even at −89 °C [9]. In addition, the research of Co_3O_4 catalysts significantly advanced metal oxides catalysing low-temperature CO oxidation [4, 11-15]. Recently, it was reported that Co_3O_4 nanorod with mainly exposed {110} planes could completely catalyse CO to CO_2 at as low as −77 °C [4]. Despite great advances, it is still challenging to find an approach to design an improved catalyst to achieve higher catalytic activities at low temperatures to broaden the feasible range to more extreme conditions for CO removal.

In general, the whole cycle of CO oxidation undergoes CO adsorption, the formation of active oxygen, CO reacting with active oxygen, and CO_2 desorption. Due to the competition between CO adsorption and the formation of active oxygen, an overwhelming majority of work was concentrated on addressing the difficult issue of how to balance or how to separate these two factors. For noble metal catalysts such as Pt, the low catalytic activity frequently stems from the too strong CO adsorption on its surface [16], namely CO poison effect, especially at low temperatures, which blocks the active sites for oxygen adsorption and activation. Unlike Pt catalyst, the nano-Au surface can more weakly chemisorb CO, resulting in the excellent catalytic activity of the nano-Au for low temperature CO oxidation [5, 8, 17]. In addition, a method for providing the extra active sites of oxygen activation on the catalyst can be adopted to improve the catalytic activity of noble metals for CO oxidation. For instance, growing FeO_x on Pt (111) could supply the extra active sites for O_2 activation for Pt catalyst with the help of FeO_x [18]. For the metal oxide catalysts (e.g. Co_3O_4) used in the CO oxidation, the increase of CO adsorption sites or the enhancement of O_2 activation is usually adopted to improve the activity of CO oxidation. For instance, the amount of CO adsorption sites could be increased by controlling the morphology or particle size of catalyst,[4, 19, 20] and the use of pre-treatments on catalysts can produce more oxygen vacancies [11, 21, 22].

However, it should be noted that the coupling of adsorbed CO with activated O and the desorption of CO_2, which were overlooked for the whole process, could also be of key importance to the reactivity. In order to make further breakthroughs on CO oxidation, in this work we take a novel approach based on the following rational: except for sufficient CO adsorption and effective O_2 activation which were extensively investigated, a good catalyst for CO oxidation at low temperature should also meet the demands: low energy barrier of CO reacting with active oxygen which requires both low CO adsorption energy and active oxygen, and rapid CO_2 desorption for avoiding the accumulation of surface carbonate species which would severely impair the catalytic activity for metal oxide catalysts [4, 23, 24]. Both of these demands are correlated to low CO adsorption strength. Hence, based on the comprehensive consideration of the factors above, low but sufficient CO adsorption energy and enough active oxygen are crucial to the design of the improved catalyst. To this end, we design a novel catalyst by weakening the CO adsorption to some extent on Co_3O_4 surface and decreasing the formation energy of oxygen vacancy simultaneously.

The doping of metal cations is a very useful method to improve the performances of catalysts [12, 13, 25-28]. For CO oxidation, we need to consider the following issues. To improve the catalytic performance of Co_3O_4 catalysts, the dopant (M) is firstly expected to possess a weaker M-O bonding than that of Co-O in order to decrease the oxygen vacancy formation energy. Secondly, a cation with relatively larger radius is also desired, which could distort the structure to make the formation of oxygen vacancy easier. Thirdly, it is better that the dopant should make Co cations lose less electrons to oxygen, which can lower the d-band center of Co to decrease CO bonding. With these considerations, we suggest that indium may be a promising candidate, meeting the demands mentioned above.

Based on our rational above, we design and prepare In_2O_3-Co_3O_4 catalyst for CO oxidation in this work. Surprisingly, this catalyst can achieve complete oxidation of CO at −105 °C and

50% conversion at −115 °C. To the best of our knowledge, this is the first study reporting CO oxidation breaking through the limit of −100 °C, which makes it possible to broaden the feasible range to more extreme conditions for CO removal.

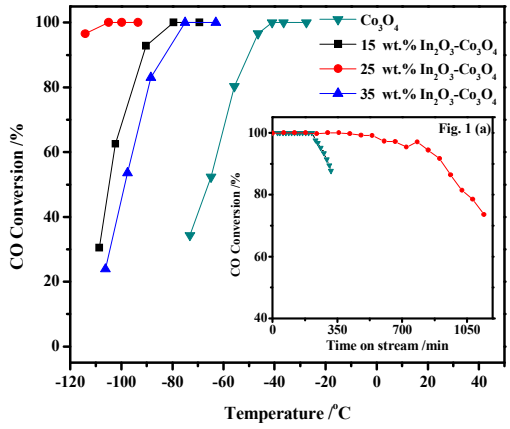

Fig. 1. The catalytic activity of Co_3O_4 and In_2O_3-Co_3O_4 samples and (inset) the catalytic stability of 25 wt.% In_2O_3-Co_3O_4 and Co_3O_4 for CO oxidation at 0 °C.

Fig. 1 shows the catalytic activity of Co_3O_4 and In_2O_3-Co_3O_4 samples for CO oxidation under the condition of 20 vol.% O_2, 1 vol.% CO and N_2 balanced in the dry feed gas and the space-velocity is 15,000 ml/h•g_{cat}. As expected, the presence of In_2O_3 can significantly promote the catalytic activity of Co_3O_4, and the lowest temperature of complete conversion (LTCC) of CO is as low as −105 °C over 25 wt.% In_2O_3-Co_3O_4 catalyst, while the corresponding LTCC is −40 °C over pure Co_3O_4. The TOF value at −75 °C over 25 wt.% In_2O_3-Co_3O_4 is about 1.7×10^{-7} mol/s•m^2, and TOF on the pure Co_3O_4 is only 3.2×10^{-8} mol/s•m^2. Furthermore, the activity of 25 wt.% In_2O_3-Co_3O_4 is further promoted by increasing the concentration of O_2 or decreasing the concentration of CO. For instance, LTCC of CO can reach −115 °C when the concentration of CO is 0.5 vol.%, or 30 vol.% O_2 is used (Table. S1).

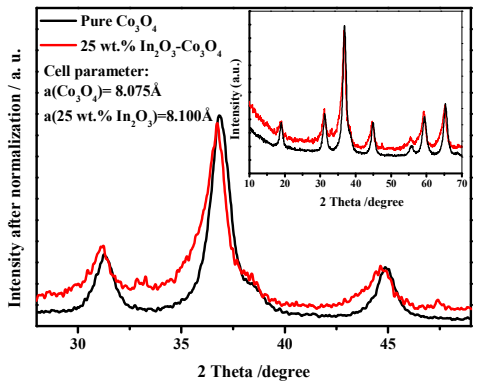

Fig. 2. The XRD patterns of pure Co_3O_4 and 25 wt.% In_2O_3-Co_3O_4.

In the XRD pattern of 25 wt.% In_2O_3-Co_3O_4 catalyst (Fig. 2), only the characteristic peaks of Co_3O_4 can be detected, which shift to lower degrees and become broader. In terms of XRD results, the fitted cell parameter of Co_3O_4 in 25 wt.% In_2O_3-Co_3O_4 (a = 8.100 Å) is larger than that of pure Co_3O_4 (a = 8.075 Å), which indicates that the In cations with larger radius are inserted into the lattice of Co_3O_4, resulting in the lattice expansion. The Raman spectra (Fig. S1) show that, comparing with Co_3O_4, the Raman peaks of tetrahedral sites (CoO_4) and octahedral sites (CoO_6) on 25 wt.% In_2O_3-Co_3O_4 sample shift to the lower wavenumber and are broadened, which also confirms the increase of lattice distortion and residual stress of Co_3O_4 after deposition of In_2O_3 [29]. Furthermore, the density functional theory (DFT) calculation results also show that the lattice constant (a = 8.210 Å) of In-doped Co_3O_4 is larger than that (a = 8.110 Å) of pure Co_3O_4, and the bulk structure of the In-doped Co_3O_4 is illustrated in Fig. S2. The results mentioned above suggest that In^{3+} cations have entered the lattice of Co_3O_4.

The formation energy of oxygen vacancy in bulk Co_3O_4 and doped-In Co_3O_4 were studied. The calculated formation energy (4.68 eV) of oxygen vacancy on O_{In} (oxygen adjacent to In^{3+}) sites is 0.25 eV lower than that (4.93 eV) on O_{Co} (oxygen only bonding to Co ion) sites. This implies that the oxygen activity of catalyst has been increased due to the presence of In.

The effect of doped In cations on the chemisorption of CO was also investigated. The bader charge analysis shows that O_{In} possesses more negative charges than O in pure Co_3O_4 by 0.035 e. This might be attributed to the higher electronegativity (1.88) of Co than that of In (1.78) [30], that is to say the lattice oxygen of catalyst can attract more electrons from In cations than substituted Co cations. Consequently, lattice oxygen in In-doped Co_3O_4 tends to attract fewer electrons from its adjacent Co cations to balance its excess electrons due to the doped In^{3+}. It is also found that the Co^{2+} and Co^{3+} cations adjacent to O_{In} in In-doped Co_3O_4 are slightly less positive than those in Co_3O_4. The XPS results also confirm this result; the 2p binding energies (BE) of Co^{2+} and Co^{3+} shift to lower BE by 0.40 eV and 0.25 eV, respectively, comparing to that of pure Co_3O_4 (Fig. S3).

The FT-IR spectra of CO adsorption (Fig. S4) show that the vibration absorption band of C=O bond over In-doped Co_3O_4 is blue-shifted, which indicates that the strength of CO adsorption and bond strength of C-Co are weakened. These results are in good agreement with our DFT calculation results that CO can easily adsorb on surface 5-fold Co^{3+} with a lower chemisorption energy (0.58 eV) relative to that on pure Co_3O_4 (100)-B (1.16 eV). The results above are also consistent with the change of the C-O bond length: the bond length of CO adsorbed on In-doped Co_3O_4 (100)-B surface shrinks to 1.156 Å from 1.158 Å of the C-O bond length on pure Co_3O_4 (100)-B surface. Conversely, the Co-C bond elongates to 1.779 Å from 1.768 Å on pure Co_3O_4 (100)-B, which can be attributed to the downshift of d-band center due to more electrons in Co cations after doping In cations. The details of adsorption structure are described in Fig. S5, in which the (100) facet was selected as the research model, because the (100) facet is the mainly exposed active plane for the conventional Co_3O_4 nanoparticles and the other exposed (111) facet containing only inactive Co^{2+} sites exhibits less activity [23, 31]. The Co_3O_4 (100) surface has two types of terminations denoted as Co_3O_4 (100)-A

and Co_3O_4 (100)-B, while the latter is much more energetically favoured [23]. Hence, Co_3O_4 (100)-B is used to study the CO oxidation.

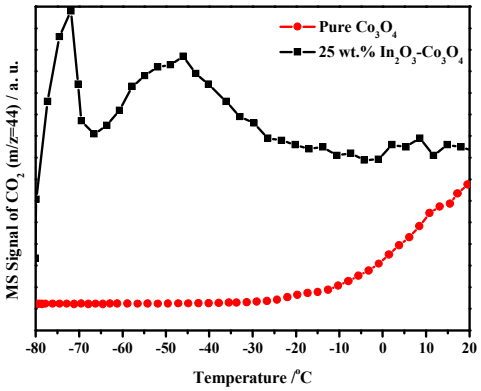

Fig. 3. The CO-TPSR profiles of 25 wt.% In_2O_3-Co_3O_4 (a) and pure Co_3O_4 (b).

Since the previous work[23, 32] has pointed out that CO reacting with lattice oxygen is slower step compared to the molecular O_2 activation followed by the formation of oxygen vacancy, the energy barrier of adsorbed CO reacting with lattice oxygen on the catalyst was mainly investigated. The reaction barrier of adsorbed CO with the oxygen adjacent to subsurface In^{3+} cation on In-doped Co_3O_4 (100)-B is only 0.33 eV, which is 0.25 eV lower than that (0.58 eV) on the pure Co_3O_4 (100)-B facet. More interestingly, this energy barrier is even lower than that on Co_3O_4 (110) facet that is the highest active surface on Co_3O_4 [4, 24]. These theoretical calculation results are confirmed by the CO-TPSR results (Fig. 3). In the CO-TPSR profiles of 25 wt.% In_2O_3-Co_3O_4 at −80~20 °C, two obvious CO consumption peaks can be observed; for pure Co_3O_4, CO is just consumed at higher than −20 °C. The H_2-TPR profiles (Fig. S6) also show that the doping of In_2O_3 obviously enhances the reducibility of Co_3O_4. These results indicate that the doping of In^{3+} makes the formation of oxygen vacancy easier and leads to a significant increase of the reactivity of surface oxygen on 25 wt.% In_2O_3-Co_3O_4, promoting its catalytic activity for CO oxidation.

The results above show that the doped In cations enter the lattice of Co_3O_4, which reduce the formation energy of oxygen vacancy and promote O_2 activation. At the same time, the presence of In also increases the electron on the Co cations and weakens the adsorption of CO on the catalyst surface. The promoted O_2 activation and weakened CO adsorption strength decrease the reaction barrier of CO oxidation, which leads to the high activity of In-doped Co_3O_4 for CO oxidation.

Generally speaking, the weaker CO adsorption is expected to weaken CO_2 adsorption, and stronger CO_2 adsorption gives easily rise to the formation of surface carbonate species, which results in a deactivation of Co_3O_4 for CO oxidation [4, 24]. The DFT results show the chemisorption energy (0.14 eV) of CO_2 on In-doped Co_3O_4 (100)-B is 0.22 eV lower than that (0.36 eV) on the pure Co_3O_4 (100)-B facet. With the help of *in-situ* DRIFT testing at −70 °C, we can see that the significant accumulation of surface carbonate species (including unidentate carbonates and bicarbonate) over pure Co_3O_4 at −70 °C can be observed (Fig. 4), and after adding In_2O_3 in Co_3O_4 the formation rate of surface carbonate species declines remarkably. The relation of the amounts of surface carbonate species formed on the surface of 25 wt.% In_2O_3-Co_3O_4 and Co_3O_4 as the function of reaction time (Fig. S7) shows that the formation rate of carbonate species on 25 wt.% In_2O_3-Co_3O_4 is about one tenth as that on pure Co_3O_4 during the initial reaction period. After reacting 20 min, the total amount of the surface carbonate species on 25 wt.% In_2O_3-Co_3O_4 is about one fifth as that on pure Co_3O_4. These results indicate that the weaker adsorption of CO_2 over In-doped Co_3O_4 inhibits the accumulation of surface carbonate species. As a result, the stability of 25 wt.% In_2O_3-Co_3O_4 is enhanced significantly and the deactivation rate is obviously inhibited. Under dry feed gas condition, the complete CO conversion can sustain at 0 °C for 210 min over pure Co_3O_4 catalyst, and using 25 wt.% In_2O_3-Co_3O_4 catalyst 100% CO conversion can sustain 600 min (Fig. 1-inset). The activity of deactivated 25 wt.% In_2O_3-Co_3O_4 and pure Co_3O_4 catalysts could be recovered completely after pretreatment in 20 vol.% O_2/N_2 at 350 °C for 40 min. For the 25 wt.% In_2O_3-Co_3O_4 catalyst, the rapid desorption of CO_2 also decreases the CO_2 solidification to block surface active sites at ultralow temperature that is lower than the CO_2 freezing point of −78.5 °C. Hence, the decrease of adsorption strength of CO obviously weakens the adsorption of CO_2, and reduces the surface carbonate species accumulation on the catalyst surface, which maintains the high activity of 25 wt.% In_2O_3-Co_3O_4 for a long time.

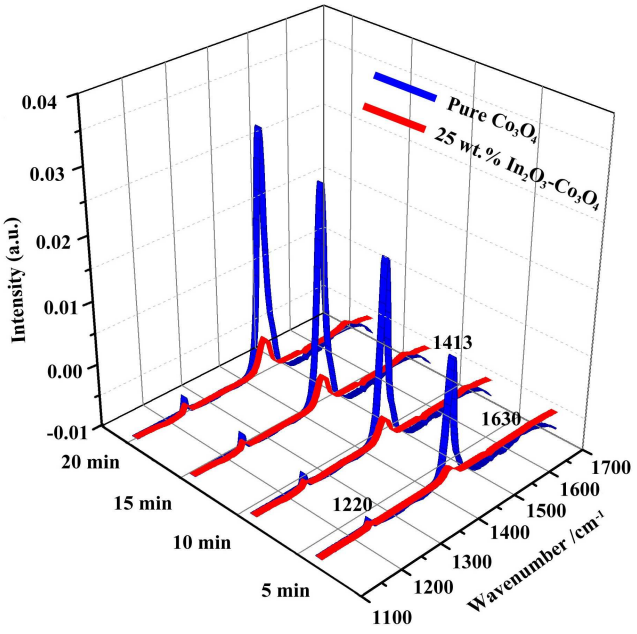

Fig. 4. *in-situ* DRIFT spectra during the CO oxidation at −70 °C over pure Co_3O_4 and 25 wt.% In_2O_3-Co_3O_4 at different reaction times in the flow of 1 vol.% CO, 20 vol.% O_2 and N_2 balanced. The bands at 1413 and 1220 cm^{-1} are ascribed to the unidentate carbonates species and the peak at 1630 cm^{-1} is attributed to bicarbonate species.

In summary, the doped In^{3+} cations can significantly improve the catalytic performance of Co_3O_4 for low-temperature CO oxidation. Under dry feed gas condition, CO can be completely converted to CO_2 at −105 °C over 25 wt.% In_2O_3-Co_3O_4. Both experimental and theoretical calculation results demonstrate that the presence of In^{3+} in Co_3O_4 can simultaneously tune the adsorption strength of CO and reactivity of oxygen species on the catalyst, which gives rise to the extraordinarily high catalytic activity. The doping of metal cations with lower M-O bonding energies, larger cation radii and relatively lower electronegativity may be a very useful approach to design the highly efficient doped Co_3O_4 catalyst. Furthermore, the rational and strategy to develop the new catalysts in this work may be of general use to other catalytic systems.

This project was supported financially by the National Basic Research Program of China (2010CB732300, 2013CB933201), the National High Technology Research and Development Program of China (2011AA03A406), NSFC of China (21171055, 21273150, 21333003, 21303051), the New Century Excellent Talents in University (NECT-10-0377), Shanghai Natural Science Foundation (13ZR1453000) and Fundamental Research Funds for the Central Universities. The authors thank National Supercomputer Center in Jinan for computing time.

Notes and references

[a] *Key Labs for Advanced Materials, Research Institute of Industrial Catalysis, East China University of Science and Technology, 130 Meilong Road, Shanghai 200237, China. (+) 86-21-64253703; E-mail: yunguo@ecust.edu.cn*

[b] *School of Chemistry and Chemical Engineering, The Queen's University of Belfast, Belfast, BT9 5AG, UK.*

[+]*These authors contributed equally to this work*

† Electronic Supplementary Information (ESI) available: [The details of characterizations and density functional theory calculations; the CO oxidation activities under the different conditions; the DRIFT spectra of CO adsorption and surface carbonate species; and Supplementary References.]. See DOI: 10.1039/b000000x/

1 Corti, C. W., Holliday, R. J., Thompson, D.T., Top. Catal. 2007, **44**, 331.
2 Valden. M.; Lai, X.; Goodman, D. W. Science. 1998, **281**, 1647.
3 Chen, M. S.; Goodman, D. W. Science. 2004, 306, 252.
4 Xie X. W.; Li Y.; Liu Z. Q.; Haruta M.; Shen W. J. Nature. 2009, **458**, 746.
5 Haruta, M.; Yamada, N.; Kobayashi, T.; Iuima, S. J. Catal. 1989, **115**, 301.
6 Li, S. Y.; Liu, G.; Lian, H. L.; Jia, M. J.; Zhao, G. M.; Jiang, D. Z.; Zhang, W. X. Catal. Commun. 2008, **9**, 1045.
7 Shen, Y. X.; Lu, G. Z.; Guo, Y.; Wang, Y. Q. Chem. Commun. 2010, **46**, 8433.
8 Haruta, M.; Tsubota, S.; Kobayashi, T.; Kageyama, H.; Genet, M.J.; Delmon, B. J. Catal. 1993,**144**, 175.
9 Jia, C. J.; Liu, Y.; Bongard, H.; Schüth, F. J. Am. Chem. Soc. 2010, **132**, 1520.
10 Green, I. X. Y., Tang, W. J., Neurock, M., Yates, J. T. Science. 2011, **333**, 736-739.
11 Yu, Y. B.; Takei, T.; Ohashi, H.; He, H.; Zhang, X.; Haruta, M. J. Catal. 2009, **267**, 121.
12 Lou, Y.; Wang, L.; Zhang, Y. H.; Zhao, Z. Y.; Zhang, Z. G.; Lu, G. Z.; Guo, Y. Catal. Today. 2011, **175**, 610.
13 Lou, Y.; Wang, L.; Zhao, Z. Y.; Zhang, Y. H.; Zhang, Z. G.; Lu, G. Z.; Guo, Y.; Guo, Y. L. Appl. Catal. B: Environmental. 2014, **146**, 43.
14 Cunningham, D. A. H.; Kobayashi, T.; Kamijo, N.; Haruta, M. Catal. Lett. 1994, **25**, 257.
15 Thormählen, P. J. Catal. 1999, **188**, 300.
16 Bourane, A.; Bianchi, D. J. Catal. 2004, **222**, 499.
17 Haruta, M. Gold Bulletin. 2004, **37**, 27.
18 Fu, Q.; Li, W. X.; Yao, Y. X.; Liu, H. Y.; Su, H. Y.; Ma, D.; Gu, X. K.; Chen, L. M.; Wang, Z.; Zhang, H.; Wang, B.; Bao. X. H. Science. 2010, **328**, 1141.
19 Hu, L. H.; Sun, K. Q.; Peng, Q. Xu, B. Q.; Li. Y. D. Nano Research. 2010, **3**, 363.
20 Tüysüz, H.; Comotti, M.; Schüth, F. Chem. Commun. 2008, **34**, 4022.
21 Wang, Y. Z.; Zhao, Y. X.; Gao, C. G.; Liu, D. S. Catal. Lett. 2008, **125**, 134.
22 Jansson, J.; Palmqvist, A. E. C.; Fridell, E.; Skoglundh, M.; Österlund, L.; Thormählen, P.; Langer, V.; J. Catal. 2002, **211**, 387.
23 Wang, H. F.; Kavanagh, R.; Guo, Y. L.; Guo, Y.; Lu, G. Z.; Hu, P. J. Catal. 2012, **296**, 110.
24 Wang, H. F.; Kavanagh, R.; Guo, Y. L.; Guo, Y.; Lu, G. Z.; Hu, P. Angew. Chem. Int. Ed. 2012, **51**, 6657.
25 Chen, H. Y.; Sayari, A.; Adnot, A.; Larachi, F.; Appl. Catal. B: Environmental 2001, **32**, 195.
26 Li, Y.; Fu, Q.; Flytzani-Stephanopoulos, M. Appl. Catal. B: Environmental. 2000, **27**, 179.
27 Liu, Y.; Wen, C.; Guo, Y.; Lu, G. Z.; Wang, Y. Q. J. Phys. Chem. C. 2010, **114**, 9889.
28 Shapovalov, V.; Metiu, H. J. Catal. 2007, **245**, 205.
29 Lopes, I.; Hassan, N. E.; Guerba, H.; Wallez, G.; Davidson, A. Chem. Mater. 2006, **18**, 5826.
30 Huheey, J. E., Keiter, E. A., Keiter, R. L., Inorganic Chemistry : Principles of Structure and Reactivity. 4th edition New York, USA: HarperCollins; 1993.
31 Pang, X. Y., Liu, C., Li, D. C., Lv, C. Q., Wang, G. C. Chemphyschem. 2013, **14**, 204.
32 Jiang, D. E., Dai, S. Phys. Chem. Chem. Phys. 2011, **13**, 978.